Optimal geothermometry and geobarometry

ROGER POWELL

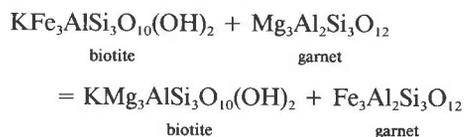Department of Geology, University of Melbourne, Victoria 3052, Australia

TIM HOLLAND

Department of Earth Sciences, University of Cambridge, Cambridge, U.K.
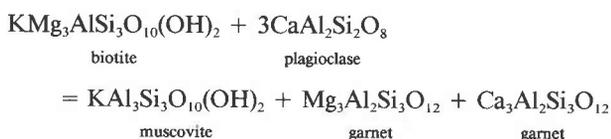
ABSTRACT

With the existence of thermodynamic data for a wide range of end-members in rock-forming minerals, thermobarometry now involves combining many equilibria to find the pressure and temperature (P-T) of formation of a rock. We reiterate that this task need only involve an independent set of reactions representing all these equilibria. In finding a P-T of formation, there is an implied displacement of the equilibria to coincide with this P-T. These displacements are mainly made by varying the activities of the end-members of the minerals, in proportion to their uncertainties. As a consequence, the equilibria are constrained to move in a more or less highly correlated way because the equilibria involve overlapping subsets of the end-members. These essential correlations should be included in any thermobarometry calculations. Of the three thermobarometry approaches in use, the TWEEQU approach of Berman (1991), the individual species approach of Gordon (1992), and our average P-T approach, only the last two are optimal on this basis. In addition, such optimal approaches allow P-T, their uncertainties, and a range of diagnostics for outlier identification to be calculated in a computationally straightforward way.

INTRODUCTION

The application of thermometry and barometry to metamorphic rocks has become increasingly sophisticated in recent years. Early applications used single reactions, written to relate a small group of mineral end-members and calibrated by direct experimental investigation. Popular reactions of this sort include the exchange of Fe and Mg between garnet and biotite as a thermometer (e.g., Reaction 5, Fig. 1a):

$$KFe_3AlSi_3O_{10}(OH)_2 + Mg_3Al_2Si_3O_{12}$$

      biotite   garnet

$$= KMg_3AlSi_3O_{10}(OH)_2 + Fe_3Al_2Si_3O_{12}$$

        biotite   garnet

together with a pressure-dependent reaction such as the Ghent and Stout barometer (Reaction 7, Fig. 1a) (Ghent and Stout, 1981):

$$KMg_3AlSi_3O_{10}(OH)_2 + 3CaAl_2Si_2O_8$$

    biotite   plagioclase

$$= KAl_3Si_3O_{10}(OH)_2 + Mg_3Al_2Si_3O_{12} + Ca_3Al_2Si_3O_{12}$$

    muscovite   garnet   garnet

to determine a unique P and T for a rock containing the assemblage garnet + biotite + muscovite + plagioclase + quartz. This approach to thermometry and barometry leads ultimately to a large library of standard calibrated reactions (as, for example, in the review of Essene, 1989). A further refinement is to seek additional reactions that are not experimentally determined but whose P-T loca-

tions may be readily determined by suitable linear combinations of reactions that do have a secure experimental base. Often this refinement is performed by manually combining the thermodynamic equilibrium relations that have been fitted to the individual experiments (e.g., Ghent et al., 1979), but it is becoming more common to do it using an internally consistent thermodynamic data set (e.g., Powell, 1978; Helgeson et al., 1978; Holland and Powell, 1985, 1990; Berman, 1988). The advantage of the latter approach is that all available experimental information, rather than just a selected subset, is used in evaluating the P-T locations of the chosen reactions. With more than one thermometer and barometer for a particular mineral assemblage, the system becomes overdetermined, and some method is required for finding the best P-T. This situation was first investigated by Powell (1985a), who advocated a least-squares method for averaging the calculated pressures for an independent set of reactions for a rock representing all the available equilibria, incorporating the uncertainties in and correlations of the calculated pressures. This approach has since been refined and developed (Powell and Holland, 1988, and in the software, Thermocalc, rev. 1990: Powell and Holland, 1988). We call this the average P-T method. The importance of overdetermined systems has now been recognized in the literature, and several papers have been published recently with the aim of optimizing pressure and temperature estimation for rocks (Gordon, 1992; Berman, 1991). As outlined below, the approach advocated by Gordon (1992) is essentially identical to ours,

but the TWEEQU approach of Berman (1991) does not make full use of the information available, and so cannot be guaranteed to yield optimal results. In this paper, we describe the average P-T method and, in particular, show how useful diagnostics relating to the dependence of the calculated P-T on the input data may be obtained.

RELATIONSHIPS WITH CONVENTIONAL THERMOBAROMETRY

To consider relationships with conventional thermobarometry, the rock RP13, which has been used in previous discussions (Powell, 1985a; Powell and Holland, 1988; Holland and Powell, 1990; Berman, 1991) is revisited. RP13 is a lower amphibolite facies calc-pelite from Spean Bridge, Inverness-shire, Scotland (Richardson and Powell, 1976), with an assemblage of quartz + oligoclase + muscovite + biotite + chlorite + garnet + epidote + calcite. Figure 1 shows the situation often encountered where one barometer, such as the shallow dP/dT Ghent and Stout barometer (Reaction 7, Table 1), and one thermometer, such as the steep dP/dT garnet-biotite thermometer (Reaction 5, Table 1), are used to estimate the pressure and temperature point of equilibration of the mineral assemblage. The thermodynamics for each reaction can usually be expressed, for a more or less restricted range in P and T, as a simple linear equation of the form $\Delta G^0 = a + bT + cP$, which, with $-\Delta G^0 = RT \ln K$, can be rearranged as $T = -(a + cP)/(b + R \ln K)$ to give the straight line form seen in Figure 1. The uncertainties in each reaction stem from errors in the thermodynamic data (principally from the enthalpies of the end-members), from imprecision in the determination of mineral compositions (e.g., from microprobe errors), and from poorly known activity-composition relationships. The first source of uncertainty is often less important than the second and third in most practical applications. It is straightforward to propagate these uncertainties to the reactions as bands in P-T space (explained below and in Powell and Holland, 1988). The uncertainty in the joint P-T determination is shown in Figure 1a as an ellipse that is tangent to, and inscribed within, the polygon of intersection of these uncertainty bands (Powell and Holland, 1988). The width of the uncertainty bands and the size of the ellipse depend on the required level of certainty in the position of the reactions and their intersection.

In many circumstances, the petrologist is fortunate enough to find more than two independent thermobarometers, and thus has some chance of determining the reliability of his result by examining the degree of consistency among the estimates from the three (or more) equilibria. Consider the situation where a third reaction may be written for the assemblage discussed in Figure 1a. Reaction 9 (Table 1) may be said to be in agreement with Reactions 5 and 7 of Table 1 if their uncertainty bands overlap. If that is so, then there exists, in some statistical sense, a unique pressure and temperature (for example, the point $\overline{P}$-$\overline{T}$ in Fig. 1b), which will lie within the uncertainty interval of all three reactions. Then a solution
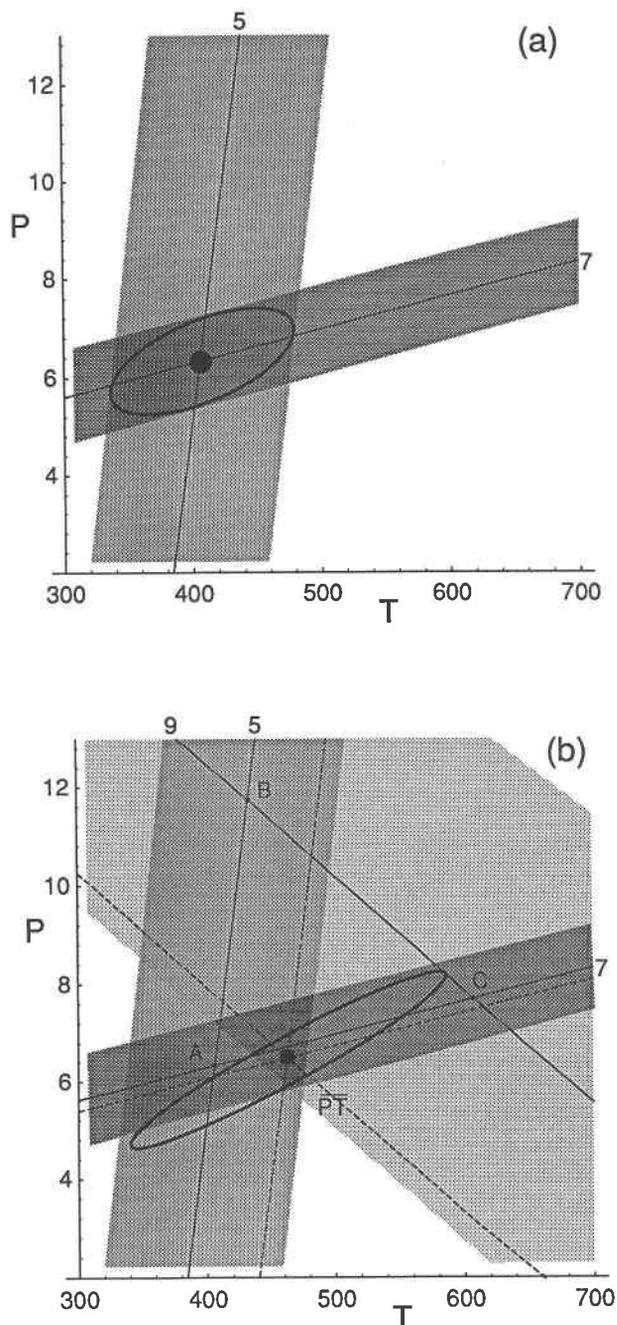

Fig. 1. (a) Intersection of two reactions from Table 1 to generate a P-T uncertainty ellipse. Reaction 7 has a smaller uncertainty than Reaction 5. This example is taken from rock RP13, using Thermocalc and data in Table 4. (b) The effect of adding a third independent Reaction 9, with a large uncertainty is to generate three intersections A, B, and C. The optimal P-T calculated by Thermocalc, shown as the spot marked $\overline{P}$-$\overline{T}$, lies within the consistent region where all three uncertainty bands overlap. The correlated uncertainties in Reactions 5, 7, and 9 (and hence in A, B, and C) cause the optimal P-T to lie outside the triangle ABC, and to have a highly flattened uncertainty ellipse, implying that pressure is well determined if a good estimate of temperature can be made.

TABLE 1. Reactions and calculated pressures for the RP13 subset used by Berman (1991, Fig. 3 of that paper)

n	Mu	Phl	Ann	Clin	Gr	Py	Alm	An	Cz	Q	P	σ_P
1	0	5	−5	−3	−5	0	5	−33	24	3	7.39	0.58
2	5	0	−5	−3	0	5	5	−48	24	3	7.32	0.46
3	5	−5	0	−3	0	10	0	−48	24	3	6.88	0.51
4	5	5	−10	−3	0	0	10	−48	24	3	7.74	0.48
5	0	1	−1	0	0	−1	1	0	0	0	31.07	10.52
6	1	0	−1	0	1	0	1	−3	0	0	8.37	0.73
7	1	−1	0	0	1	1	0	−3	0	0	7.18	0.94
8	11	0	−11	3	16	−5	11	0	−24	−3	14.67	3.85
9	11	−11	0	3	16	6	0	0	−24	−3	9.49	5.88
10	11	−5	−6	3	16	0	6	0	−24	−3	12.66	4.43
11	5	−5	0	3	10	0	0	18	−24	−3	6.17	1.5
12	0	0	0	3	5	−5	0	33	−24	−3	6.72	0.54

Note: temperature was at 530 °C and $x_{CO_2} = 0.25$. Of the pairs of pressures, 25% are more correlated than ±0.75.

is sought to the problem of determining this optimal P-T position, as well as its uncertainty ellipse. This is not as straightforward as it appears, because an appropriate method is needed for averaging the three (or more) P-T points whose positions are, in general, highly correlated with each other and whose uncertainties are far from equal. In general, simple averaging of the P-T points does not yield the correct result, even when each P-T point is assigned some notional weight. The main purpose of this paper is to establish an appropriate method of averaging, as well as to discuss other recent developments in this field (Berman, 1991; Gordon, 1992).

THE AVERAGE P-T METHOD

Averaging the equilibria for a rock to obtain an optimal P-T can be viewed as essentially a statistical problem. The input data, particularly the activities of the end-members, are uncertain, and the way these uncertainties propagate controls the position of the calculated P-T. The way uncertainties in activities of mineral end-members propagate through to ln K and thus to P-T is outlined first. That is followed by a discussion of the use of independent sets of reactions in calculations, and then the average P-T method itself is outlined.

Uncertainties and correlations

In considering the way uncertainties in activities propagate to ln K, it is important to understand that, although the individual end-member activities may usually be taken to be independent and therefore uncorrelated, ln K values are generally correlated. In fact, as soon as two reactions involve any of the same (uncertain) end-members, the ln K values are correlated. Such correlations propagate through to correlations between the P-T positions of intersections. Thus, because intersections such as A, B, and C in Figure 1b have mineral end-members in common, any changes to a particular end-member activity lead to correlated displacements in the locations of these three P-T points: a change in activity of one end-member will lead to movement of all the points involving that end-member in a readily predictable way. It is therefore ab-

solutely essential to take such correlations into account if the positions of many equilibria are to be combined to calculate an overall P-T. The correlations are part of the fundamental structure of the problem.

To illustrate the behavior of uncertainties, we consider the equilibria in hypothetical high-pressure rocks containing the assemblage jadeite + paragonite mica + kyanite coexisting with quartz and plagioclase. Two independent reactions in the model system Na_2O-Al_2O_3-SiO_2-H_2O may be written

$$jd + q = ab \qquad (1)$$

$$pa + q = ab + ky + H_2O. \qquad (2)$$
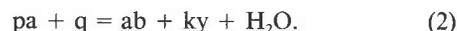
Denoting the equilibrium constants of these two reactions, ln K_1 and ln K_2, the correlated uncertainties can be represented as in Figure 2a, with the correlation, and thus the shape of the ellipse, depending on the sources of uncertainty. If the only mineral showing a solid solution is plagioclase feldspar, then the activity of albite and its uncertainty lead to a perfect positive correlation between the equilibrium constants for the two reactions because 1 mol of albite occurs on the right side of each. Thus ln $K_1 = $ ln $K_2 = $ ln a_{ab}. A change in albite activity causes an identical shift in the value of ln K for both reactions, and hence the joint uncertainty region (Fig. 2b) is a line, as the K values are perfectly correlated. If plagioclase is pure albite, and the rock contains jadeite and paragonite solid solutions, then ln $K_1 = $ −ln a_{jd} and ln $K_2 = $ ln a_{pa}. Therefore the two values of ln K are uncorrelated, giving a joint uncertainty region (Fig. 2c) whose principal axes lie parallel to the edges of the error box. A third example intermediate between the two extremes of perfect and zero correlation occurs if the assemblage involves solid solutions of plagioclase and jadeite with pure paragonite where ln $K_1 = $ ln a_{ab} − ln a_{jd} and ln $K_2 = $ ln a_{ab}; in this case the two ln K values are correlated by their sharing albite, but the presence of jadeite in Reaction 1 allows some independent uncertainty variation, resulting in a joint uncertainty region (Fig. 2a), which is a rotated and flattened ellipse. The correlation coefficients ρ_{jl} may be determined from the variances and covariances using the error propagation equations (Powell and Holland, 1988, p. 177)

$$\sigma^2_{\ln K_j} = \sum_{i=1} \left(\frac{r_{ij}}{a_{ij}}\right)^2 \sigma^2_{a_i}$$

$$\sigma_{\ln K_j \ln K_l} = \sum_{i=1} \left(\frac{r_{ij}}{a_{ij}}\right)\left(\frac{r_{il}}{a_{il}}\right)\sigma^2_{a_i}$$

where $\sigma_{\ln K_j}$ is the uncertainty in $\ln K$ for reaction j, σ_{a_i} is the uncertainty in activity of end-member i, r_{ij} is the reaction coefficient of i in reaction j, and a_{ij} is the activity of i in reaction j. The correlation coefficients, $\rho_{\ln K_j \ln K_l}$, are given by

$$\rho_{\ln K_j \ln K_l} = \frac{\sigma_{\ln K_j \ln K_l}}{\sigma_{\ln K_j}\sigma_{\ln K_l}}.$$

Such correlated errors in $\ln K$, in turn, propagate to P-T intersections, and the error propagation equation may again be used. For the intersection of two reactions, Equations 1 and 2, the thermodynamics may be written in simple form as $0 = a_1 + b_1 T + c_1 P + RT \ln K_1$ and $0 = a_2 + b_2 T + c_2 P + RT \ln K_2$; the pressure P_i, and temperature, T_i, of the intersection are given by

$$P_i = \frac{a_2(b_1 + R \ln K_1) - a_1(b_2 + R \ln K_2)}{c_1(b_2 + R \ln K_2) - c_2(b_1 + R \ln K_1)}$$

$$T_i = \frac{c_1 a_2 - a_1 c_2}{c_2(b_1 + R \ln K_1) - c_1(b_2 + R \ln K_2)}. \quad (3)$$

With the assumption that the errors only come from the uncertainties and correlations on $\ln K$, application of the error propagation equation yields the uncertainties on the P-T of the intersection:

$$\sigma^2_{P_i} = \sigma^2_{\ln K_1}\left(\frac{\partial P_i}{\partial \ln K_1}\right)^2 + \sigma^2_{\ln K_2}\left(\frac{\partial P_i}{\partial \ln K_2}\right)^2$$

$$+ 2\sigma_{\ln K_1 \ln K_2}\left(\frac{\partial P_i}{\partial \ln K_1}\right)\left(\frac{\partial P_i}{\partial \ln K_2}\right)$$

$$\sigma^2_{T_i} = \sigma^2_{\ln K_1}\left(\frac{\partial T_i}{\partial \ln K_1}\right)^2 + \sigma^2_{\ln K_2}\left(\frac{\partial T_i}{\partial \ln K_2}\right)^2$$

$$+ 2\sigma_{\ln K_1 \ln K_2}\left(\frac{\partial T_i}{\partial \ln K_1}\right)\left(\frac{\partial T_i}{\partial \ln K_2}\right) \quad (4)$$

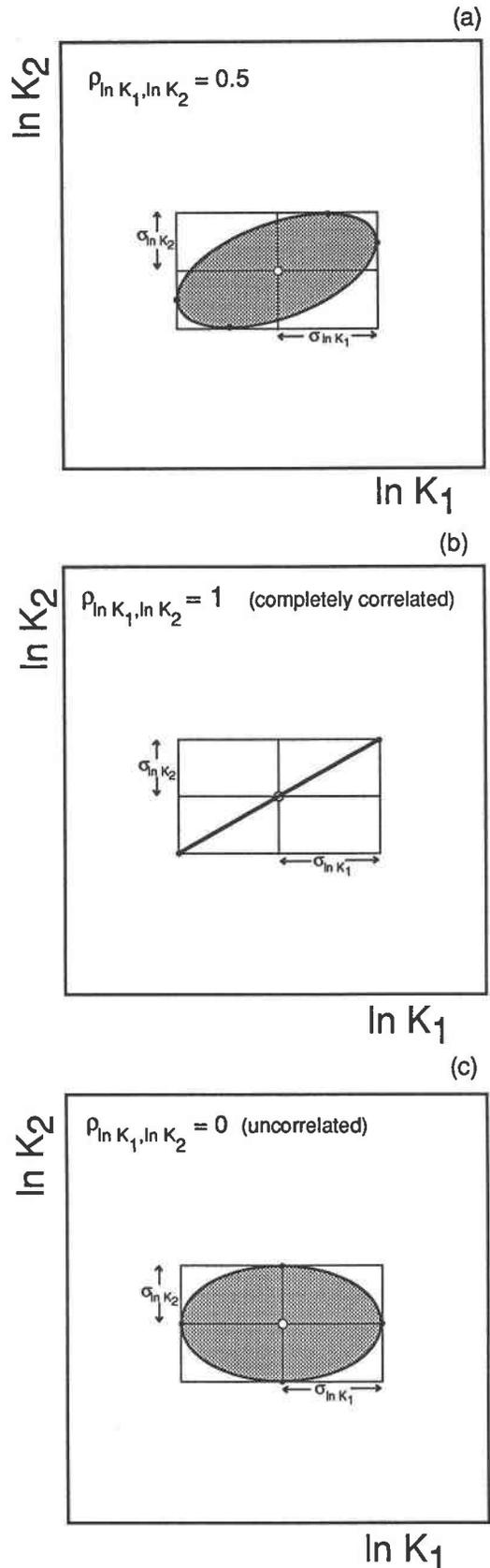and the covariance between the P and T:

$\longrightarrow$

Fig. 2. The effect of correlated uncertainties on $\ln K_1$ and $\ln K_2$. (a) The general case yields an ellipse touching the uncertainty box at points defined by the correlation coefficient $\rho_{\ln K_1 \ln K_2}$ (see Powell and Holland, 1988, their Fig. 2). Two extreme cases of correlation are illustrated in b and c. In the first case (b), with perfect correlation, $\rho_{\ln K_1 \ln K_2} = 1$, the ellipse has flattened onto its major axis, which defines a line along the diagonal of the uncertainty box; in the second case (c), with zero correlation, $\rho_{\ln K_1 \ln K_2} = 0$, the principal axes of the uncertainty ellipse are parallel to the uncertainty box. The probability of lying within a 1σ ellipse is 0.39 and within a 2σ ellipse is 0.9.

(a) $\rho_{\ln K_1, \ln K_2} = 0.5$

(b) $\rho_{\ln K_1, \ln K_2} = 1$ (completely correlated)

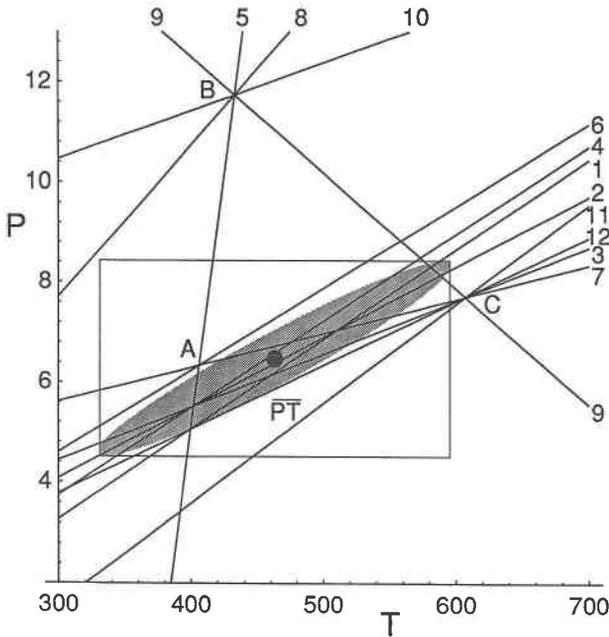(c) $\rho_{\ln K_1, \ln K_2} = 0$ (uncorrelated)

Fig. 3. The RP13 subset, shown in Table 1, omitting H_2O and CO_2 used by Berman (1991, Fig. 3 of that paper). This figure differs slightly from that of Berman because the thermodynamic data used have been updated since the paper of Holland and Powell (1990). It shows not only the three independent reactions (Fig. 1) and the optimal P-T point with its uncertainty box and ellipse, but also all 12 equilibria in the subset. It may be seen, qualitatively, that the orientation of the ellipse is partly constrained by the family of well-determined equilibria subparallel to its major axis. All reactions associated with point B have large uncertainties (e.g., see Fig. 1) and hence contribute little to the determination of P-T.

$$\sigma_{P_iT_i} = \sigma_{\ln K_1}^2 \left(\frac{\partial P_i}{\partial \ln K_1}\right)\left(\frac{\partial T_i}{\partial \ln K_1}\right) + \sigma_{\ln K_2}^2 \left(\frac{\partial P_i}{\partial \ln K_2}\right)\left(\frac{\partial T_i}{\partial \ln K_2}\right)$$
$$+ \sigma_{\ln K_1 \ln K_2}\left(\frac{\partial T_i}{\partial \ln K_1}\right)\left(\frac{\partial T_i}{\partial \ln K_2}\right)\left(\frac{\partial P_i}{\partial \ln K_1}\right)\left(\frac{\partial P_i}{\partial \ln K_2}\right).$$

$$(5)$$

The correlation between the P and T can then be calculated from:

$$\rho_{P_iT_i} = \frac{\sigma_{P_iT_i}}{\sigma_{P_i}\sigma_{T_i}}.$$

Note that, in general, P_i and T_i are correlated ($\rho_{P_iT_i} \neq 0$) even if the ln K values are uncorrelated ($\sigma_{\ln K_1 \ln K_2} = 0$). The shape of the uncertainty ellipse depends on the correlation coefficient, $\rho_{P_iT_i}$, with ellipses being less flattened as $\rho_{P_iT_i} \rightarrow 0$ and becoming extremely flattened as $\rho_{P_iT_i} \rightarrow \pm 1$, with the main axis of the ellipse having positive slope for positive correlations and negative for negative (Fig. 2).

Equations 4 and 5 would normally be extended to include the uncertainties in and, in this case, the correlations between the enthalpies of formation of the mineral

end-members calculated during the generation of the internally consistent data set used. However, our experience is that in many cases the uncertainties and correlations in such calculations derive mainly from uncertainties on the activities (Powell and Holland, 1988, p. 190; Berman, 1991, p. 836).

It is important to note that, although the above development is straightforward for well-known, normally distributed uncertainties, the approach is still valid and valuable even if the uncertainties do not have those attributes. In practice, the uncertainties on activities may come from several sources, only some of which are quantifiable. Moreover, the probability distributions may not be normal, or even symmetric, although there is no reason to suppose that asymmetry will be extreme. Regardless of these difficulties, error propagation can certainly be applied if the data are not normally distributed (e.g., Mikhail, 1976, p. 105), and, even if the magnitudes of the uncertainties are poorly known, they certainly cannot be ignored. It should be added that using Equation 4 to give $\pm$ values, for example as 2σ, is strictly only correct for normally distributed uncertainties.

Whereas the results embodied in Equations 4 and 5 give the uncertainties on the position of intersection of two reactions and thus give the P-T of a rock if only two independent reactions are being considered (as in Fig. 1a), the situation is clearly more complicated for a combination of three or more reactions (as in Fig. 1b). In this case no simple closed expressions, comparable with Equations 4 and 5, can be written, but it is obvious that the resulting P-T calculated from many equilibria will depend critically on the uncertainties on the activities, and, normally to a lesser extent, on the uncertainties on the thermodynamic data. Any method of combining equilibria that does not explicitly take the uncertainties into account will not yield an optimal solution.

Independent sets of reactions

In considering the role of sets of independent reactions in calculating P-T, we start by noting that the three reactions in Figure 1b are just three reactions of the 12 that can be written for this subset of RP13 (Table 1 and Fig. 3). For intersection A in Figure 3, the P-T position of A is clearly fixed by any two of the three reactions involved, for example, Reactions 5 and 7, the other reaction and its thermodynamics being obtainable as a linear combination of the two reactions chosen. Somewhat less obvious is that in the full system represented by Figure 3, only three reactions are independent, and that the thermodynamics of the entire system are completely specified by these three. This can be demonstrated algebraically (Powell and Holland, 1988, Appendix 2 of that paper) and also follows from the fact that the rank of the composition matrix is the same as the number of independent reactions. The number of independent reactions is just the difference between the number of end-members being considered and the number of components needed to represent their compositions: in the RP13 subset in Figure

TABLE 2. The reactions and calculated pressures for another RP13 subset

n	Mu	Phl	Clin	Gr	Cz	An	Cc	Q	H_2O	CO_2	P	σ_P
1	-5	5	-3	-7	24	-21	-6	0	0	6	6.27	1.13
2	-15	15	-9	0	72	-84	-60	-21	0	60	6.61	1.22
3	5	-5	3	10	-24	18	0	-3	0	0	6.17	1.32
4	0	0	0	3	0	-3	-6	-3	0	6	4.93	5.08
5	5	-5	3	28	-24	0	-36	-21	0	36	5.77	2.39
6	0	0	0	0	-2	3	1	0	1	-1	6.62	0.34
7	0	0	0	3	-2	0	-5	-3	1	5	6.04	1.76
8	-5	5	-3	8	0	0	-24	-15	12	24	6.35	1.16
9	-15	15	-9	0	16	0	-32	-21	28	32	6.64	0.96
10	-15	15	-9	0	0	24	-24	-21	36	24	6.63	0.58
11	-5	5	-3	-7	12	-3	0	0	6	0	-7.69	39.49
12	-25	25	-15	-32	48	0	0	-3	36	0	8.32	4.67
13	-5	5	-3	-4	0	12	0	-3	12	0	6.82	0.6
14	-15	15	-9	0	-48	96	0	-21	60	0	6.63	0.31
15	0	0	0	3	-12	15	0	-3	6	0	6.49	0.51
16	-5	5	-3	-7	10	0	1	0	7	-1	9.15	6.82
17	-5	5	-3	-7	0	15	6	0	12	-6	6.99	0.94

Note: temperature was at 530 °C and $x_{CO_2} = 0.25$. Data used in generating Table 3. Of the pairs of pressures, 33% are more correlated than ±0.75.

3, there are ten end-members in the seven-component system K_2O-CaO-MgO-FeO-Al_2O_3-SiO_2-H_2O, and so there are three independent reactions. The choice of which three to use is not prescribed, and each delivers the same information about the system.

As outlined in the last section, the correlations are an integral part of the formulation of the problem of calculating *P-T* from a set of equilibria, and omitting them is too drastic a simplification. To illustrate the deleterious effects of ignoring the correlations between reactions in any independent reaction set, another RP13 subset is considered, Table 2 and Figure 4. For this system, only three independent reactions are required to characterize the thermodynamics of the whole system, and we have investigated all of the 596 sets of three independent reactions. The average *P-T* (and the associated statistics)

for each independent set of reactions is identical when correlations are included, whereas the calculated *P-T* and statistics calculated without incorporating the correlations are quite varied (Table 3). To illustrate this variability, Figure 5 shows histograms of the calculated *P-T* values for the 596 sets.

Computing the average *P-T*

The average *P-T* method involves using a least-squares method to determine an optimal *P-T* from the thermodynamics of the reactions in an independent set, including uncertainties and correlations on the activities and enthalpies of formation of the end-members. The use of least squares is suggested because the method has various optimal properties, such as being identical to the method of maximum likelihood for normally distributed data,

TABLE 3. Calculated pressures and temperatures for the RP13 subset of Table 2 for some randomly chosen independent sets of reactions

| Reactions			Correlations omitted						Correlations included					
r_1	r_2	r_3	$\bar{P}$	$\sigma_{\bar{P}}$	$\bar{T}$	$\sigma_{\bar{T}}$	$\rho_{\bar{P},\bar{T}}$	σ_{fit}	$\bar{P}$	$\sigma_{\bar{P}}$	$\bar{T}$	$\sigma_{\bar{T}}$	$\rho_{\bar{P},\bar{T}}$	σ_{fit}
1	2	6	6.59	0.38	529.2	18.9	0.5688	0.292	6.65	0.51	531.6	13.4	0.8257	0.354
2	3	6	6.60	0.39	530.6	18.9	0.5952	0.332	6.65	0.51	531.6	13.4	0.8257	0.354
3	5	7	6.24	1.89	534.0	34.7	0.8781	0.100	6.65	0.51	531.6	13.4	0.8257	0.354
3	5	8	6.10	1.81	527.5	28.0	0.9302	0.232	6.65	0.51	531.6	13.4	0.8257	0.354
2	3	9	6.52	0.67	529.4	10.6	0.5373	0.309	6.65	0.51	531.6	13.4	0.8257	0.354
6	8	9	6.65	0.46	531.9	10.7	0.7686	0.245	6.65	0.51	531.6	13.4	0.8257	0.354
5	9	10	6.76	2.44	532.5	36.6	0.9854	0.367	6.65	0.51	531.6	13.4	0.8257	0.354
1	5	11	6.20	1.22	532.0	34.7	0.5563	0.373	6.65	0.51	531.6	13.4	0.8257	0.354
9	10	11	6.29	2.26	524.5	35.0	0.9838	0.300	6.65	0.51	531.6	13.4	0.8257	0.354
3	5	12	6.03	1.91	526.0	43.3	0.8245	0.442	6.65	0.51	531.6	13.4	0.8257	0.354
6	10	12	6.60	0.53	528.9	14.5	0.8489	0.319	6.65	0.51	531.6	13.4	0.8257	0.354
7	8	13	7.45	1.74	545.2	26.4	0.9442	0.188	6.65	0.51	531.6	13.4	0.8257	0.354
5	7	14	7.25	1.29	547.7	32.4	0.9714	0.108	6.65	0.51	531.6	13.4	0.8257	0.354
10	12	14	6.52	1.13	527.4	25.7	0.9736	0.312	6.65	0.51	531.6	13.4	0.8257	0.354
5	10	15	6.43	1.09	527.5	23.7	0.9553	0.393	6.65	0.51	531.6	13.4	0.8257	0.354
2	3	16	6.44	0.91	532.7	25.5	-0.433	0.432	6.65	0.51	531.6	13.4	0.8257	0.354
10	11	16	5.01	3.86	496.7	70.9	0.9939	0.104	6.65	0.51	531.6	13.4	0.8257	0.354
3	4	17	6.86	1.21	538.8	28.3	0.7154	0.523	6.65	0.51	531.6	13.4	0.8257	0.354
9	11	17	6.99	1.68	533.7	23.5	0.9171	0.397	6.65	0.51	531.6	13.4	0.8257	0.354

Note: cf. Gordon, 1992, Table 2 of that paper.
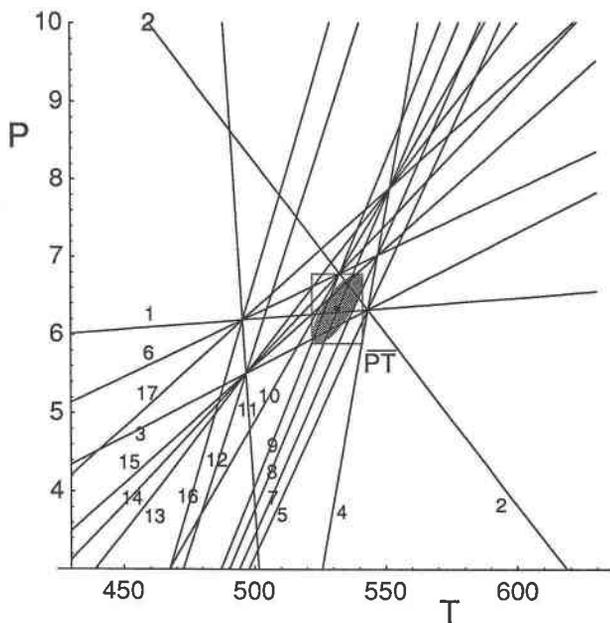
Fig. 4. The RP13 subset including H_2O and CO_2, shown in Table 2, using the data in Table 4. As in Fig. 3, there are three independent reactions, and various choices are given in Tables 2 and 3. The effect of adding H_2O and CO_2 to the subset of Fig. 3 is to constrain the P-T, particularly the temperature. The diagram is drawn for $X_{CO_2} = 0.25$. With $\sigma_{fit} = 1.54$ the χ^2 test has been passed (see text) and the various intersections displaced from the ellipse are not outliers in the sense that their uncertainties overlap those of the optimal P-T.

but it does not require that the data be normally distributed (e.g., Mikhail, 1976, p. 105).

Although average P-T calculations have been available to users of Thermocalc since 1990, the underlying method has not been published, though the average P method on which it is based was outlined in Powell (1985a) and Powell and Holland (1988). The average P-T method is needed as soon as more than two independent reactions are involved, which is the usual situation with the wide range of mineral end-members in current internally consistent data sets (e.g., Berman, 1988; Holland and Powell, 1990). For example, unprepossessing assemblages, such as albite + actinolite + chlorite + epidote + quartz, may have five or six independent reactions, and the full RP13 assemblage has 11 (with the data set of Holland and Powell, 1990). Each reaction in the independent set with the equilibrium condition $0 = \Delta G^0 + RT \ln K$ gives a relationship between pressure and temperature (and, possibly, fluid composition parameters). In addition, with the uncertainties and correlations on the input data, the positions of the reactions are uncertain, and their positions are correlated. Essentially, the least-squares method varies the positions of the reactions, in proportion to their uncertainties and correlations, so that they all intersect at one point: the average P-T. Clearly, the reactions in the independent set with the smallest uncertainty are dis-
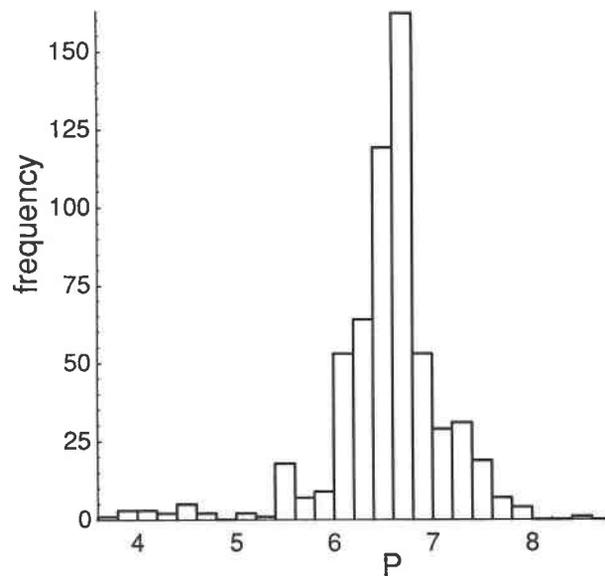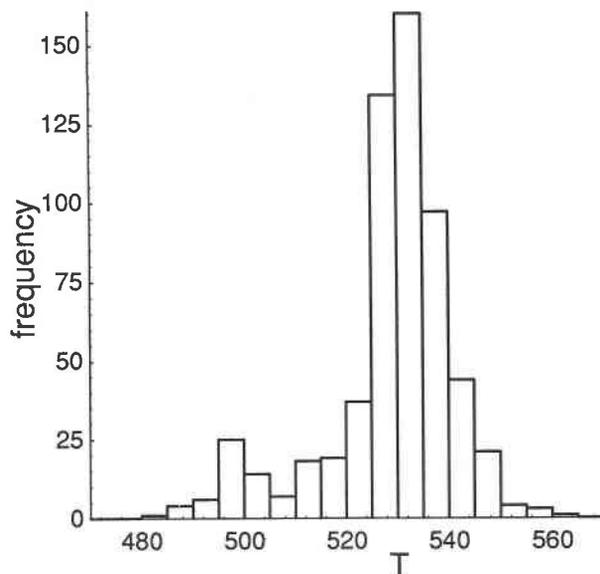

Fig. 5. The average T and average P from 596 independent sets of reactions for RP13 (see Tables 2 and 3 for examples), with uncorrelated ln K values assumed, mirroring the analysis of Gordon (1992). Note the large spread in pressures and temperatures yielded by different sets of independent reactions in the uncorrelated calculations. Incorporating the correlations in calculating the optimal P-T yields identical P and T for all the 596 independent sets.

placed least and therefore have a controlling influence on the average P-T. Moreover, the displacements in any one reaction cannot be made independently of the other reactions because such displacements are correlated through the shared end-members. Thus the average P-T method determines the optimal P-T compatible with all equilib-

ria, subject to these constraints imposed through their correlated equilibrium constants (see above).

The least-squares method for calculating average P-T, including the uncertainties and the correlations, is iterative because the equations are nonlinear. A method of doing this, as used in Thermocalc and outlined in Appendix 1, works on the activities and enthalpies of formation of the end-members and on their uncertainties and correlations. In the calculation of average P and average T, a closed form for the results is possible (e.g., Powell and Holland, 1988, p. 196–197), and, in those cases, the calculations can be performed simply from the calculated positions of the reactions, with their uncertainties and correlations, rather than requiring handling the activities and enthalpies of formation of the end-members directly. It is straightforward to show, however, that these approaches are formally equivalent. In fact, the calculation of the diagnostics discussed in a later section requires the more long-winded approach.

The average P-T is dependent on the activity uncertainties used. With a choice of activity uncertainties, the average P-T is not altered by a proportional change of all the activity uncertainties. However, for changes in activity uncertainties that are not proportional, changes to the average P-T (and their uncertainties, see below) result, the magnitudes of which depend on how the changes propagate through the calculations. The effect of changing individual uncertainties can be seen through the diagnostics discussed below. The default activity uncertainties of Powell and Holland (1988, Appendix D of that paper) are used in the calculations in this paper. Although a detailed discussion of activity uncertainties is beyond the scope of this paper, it is worth reiterating (Powell and Holland, 1988, p. 178) that there are many sources of uncertainty, not all of which are likely to be quantifiable (see also, for example, Kohn and Spear, 1991). The aim of the formulation of the default uncertainties is to provide a means of covering at least some of these sources, including those from activity model problems, in particular trying to prevent the use of uncertainties that are likely to be underestimates. Of course, if larger (or smaller) uncertainties seem to be justified, they should be used.

Estimating the uncertainties on the average P-T

Any calculation must be accompanied by an estimate of the uncertainty on the results of the calculation. The uncertainties on, and the correlations between, the calculated P and T are produced as a part of the calculation of an average P-T (Appendix 1). Note that these uncertainties are not altered by a proportional change of all the activity uncertainties, as long as the averaging is statistically consistent (by using σ_{fit} and the χ^2 test—see below). If the averaging is inconsistent, a proportional increase decreases these uncertainties until the averaging becomes consistent. For changes in activity uncertainties that are not proportional, changes to the uncertainties result. As above, the effect of changing individual uncertainties can be seen through the diagnostics below.

The uncertainties on the calculated P-T reflect how well established the P-T values are. From the (1σ) uncertainty ellipse for the RP13 subset of Figure 3, $\sigma_{\bar{P}}$ and $\sigma_{\bar{T}}$ are relatively large, but they are quite strongly correlated ($\rho_{\bar{P},\bar{T}} = 0.967$), meaning that, with a T (or P), the other value is well constrained. In comparison with the full RP13 assemblage, the omission of calcite has caused this uncertainty ellipse because reactions involving calcite act to constrain temperature. For the RP13 subset of Figure 4, which includes calcite, from the (1σ) uncertainty ellipse, $\sigma_{\bar{P}}$ and $\sigma_{\bar{T}}$ are relatively small, and so regardless of the correlation ($\rho_{\bar{P},\bar{T}} = 0.826$), both P and T are well established, at least at the chosen X_{CO_2} of 0.25.

Diagnostics

A common feature of recent discussions of thermobarometry is the desire to evaluate the quality of the calculations undertaken and particularly to investigate the influence of the input data on the calculated P-T (Powell and Holland, 1988; Berman, 1991; Lieberman and Petrakakis, 1991; Gordon, 1992). This becomes possible once the number of independent reactions involved in a calculation becomes large. Such diagnostics, which are outputted as a part of the average P-T calculations in Thermocalc, are outlined in this section (see also Tables 4–6 and Appendix 2).

Diagnostic information will be discussed with reference to an example output file from Thermocalc for rock RP13 (Table 4). The file consists of several blocks of information, the first of which is a list of end-member activities and their associated uncertainties (determined in the manner of Powell and Holland, 1988, p. 197). The second block gives the balanced independent reactions used in the calculations, with the calculated P and its uncertainty for each reaction at a specified temperature (530 °C) and fluid composition ($x_{CO_2} = 0.25$). The remaining block of information in the output pertains to the diagnostics on the calculated average P-T.

The first piece of diagnostic information to consider is σ_{fit}, a measure of the scatter in residuals (the observed minus the calculated values) of the enthalpies and activities normalized by their uncertainties, which is printed on the last line of the table summarizing the average P-T results. If the uncertainties on the input enthalpy and activity data are realistic, then the anticipated value of σ_{fit} should be close to 1.0. However, it is frequently larger than 1.0, and the χ^2 test may be used to discover whether it is close enough to 1.0 to signify that the average P-T result is consistent with the input data. In the example of Table 4, σ_{fit} is 2.02, rather larger than the maximum allowable from the χ^2 test (1.35) at the 95% confidence level. The maximum allowable σ_{fit} depends on the degrees of freedom for the problem (the difference between the number of independent reactions and the number of unknowns) and is printed by the program in the information at the head of the diagnostics table. If σ_{fit} is less than the cutoff value, then the χ^2 test has been passed, indicating that a solution for P-T has been found that is consistent

TABLE 4. Condensed Thermocalc output for the full RP13 assemblage

	Mu	Pa	Cel	Phl	Ann	East	Clin	Ames
Activities and default uncertainties								
a	0.682	0.170	0.0340	0.0774	0.0140	0.0450	0.0580	0.0270
sd(a)/a	0.10000	0.20667	0.39913	0.31259	0.51845	0.37244	0.34580	0.41902
	Daph	Gr	Py	Alm	Andr	An	Ab	Cz
a	0.00900	0.0157	9.80e-4	0.190	1.60e-4	0.561	0.640	0.650
sd(a)/a	0.56453	0.50571	0.73009	0.16265	0.80493	0.05782	0.05000	0.05000
	Ep	Cc	Q	H_2O	CO_2			
a	0.350	1.00	1.00	0.750	0.250			
Sd(a)/a	0.10007	0	0					

Reactions and calculations [for T = 530 °C, and $x(CO_2)$ = 0.25]

		$P(T)$	sd(P)
1	$2cz + CO_2 = 3an + cc + H_2O$	6.6	0.34
2	$3py + 16cz = clin + ames + 4gr + 20an$	6.6	0.58
3	$3ames + 2gr + py + 6q = 3clin + 6an$	8.0	1.35
4	$5alm + 24cz + 3q = 3daph + 5gr + 33an$	6.9	0.42
5	$cel + east = mu + phl$	8.7	24.12
6	$mu + 2phl + 6q = 3cel + py$	8.3	2.78
7	$2phl + 3ames + 6q = 2mu + 3clin + py$	4.6	3.67
8	$15cel + 12cz = 10mu + 5phl + 8gr + 27q + 6H_2O$	7.2	4.06
9	$ann + 3an = mu + gr + alm$	8.4	0.73
10	$7gr + 5alm + 24ep + 3q = 3daph + 12andr + 33an$	8.4	1.14
11	$2pa + 3cel = 2mu + phl + 2ab + 3q + 2H_2O$	4.1	1.87

Rock RP13: Average P-T [for $x(CO_2)$ = 0.25 and $x(H_2O)$ = 0.75]

Single end-member diagnostic information
(e^* cutoff = 2.8; hat cutoff = 0.52, fit cutoff = 1.35)

	P	sd(P)	T	sd(T)	Cor	Fit	e^*	Hat
Lsq	7.0	0.8	547	19	0.791	2.02		
Mu	6.99	0.77	550	19	0.783	1.96	0.90	0.03
Pa	7.12	0.59	542	14	0.766	1.50	−3.75	0.12
Cel	6.96	0.79	547	19	0.793	2.02	−0.00	0.03
Phl	7.01	0.78	550	19	0.782	1.98	−0.99	0.12
Ann	6.79	0.73	546	17	0.789	1.83	−2.66	0.05
East	6.97	0.79	548	19	0.791	2.01	−0.26	0.00
Clin	6.96	0.79	547	19	0.792	2.02	−0.15	0.03
Ames	7.04	0.77	551	19	0.791	1.95	1.45	0.07
Daph	6.91	0.84	546	20	0.818	2.01	−0.37	0.16
Gr	6.97	0.79	548	19	0.790	2.02	−0.14	0.04
Py	6.98	0.82	548	20	0.808	2.02	−0.20	0.12
Alm	6.78	0.80	543	19	0.810	1.96	1.01	0.05
Andr	6.97	0.77	549	18	0.789	1.97	−1.48	0.02
An	6.90	1.07	547	20	0.772	2.02	−0.12	0.54
Ab	6.98	0.77	547	18	0.787	1.95	0.91	0.01
Cz	7.00	0.88	548	20	0.809	2.02	−0.11	0.12
Ep	6.96	0.79	548	19	0.790	2.01	0.37	0.00
Cc	6.96	0.79	547	19	0.791	2.02	0	0
Q	6.96	0.79	547	19	0.791	2.02	0	0
H_2O	6.96	0.79	547	19	0.786	2.02	0.11	0.01
CO_2	7.01	0.82	549	20	0.803	2.01	−0.32	0.11

with the input data within their uncertainties. Lack of consistency may be caused by the errant behavior of one or more end-members (or outliers) or by a general scatter in the data, with no outliers present. In the former case, the following diagnostics may help identify the outlier end-members, which may then be removed before rerunning the program. In the latter case, with no outliers identifiable, a larger value of σ_{fit} may be acceptable if it reflects an overall underestimation of the uncertainties in the input activity data. Because the uncertainties on the average P-T have been multiplied by σ_{fit}, if the χ^2 test fails, the result in this case is larger uncertainties, to reflect the lack of consistency.

An extremely useful diagnostic, printed in the last col-umn of the table of diagnostics, the so called hat value, h_k, for each end-member, k, is a direct measure of the degree of infuence of that end-member on the least-squares result (Belsley et al., 1980, p. 16 et seq.). Hat values give an indication of how far a particular datum lies from the center of the data spread. End-members with large hat values have a controlling influence in that perturbations in their activities propagate to large changes in the final average P-T. Hat values can lie in the range 0.0–1.0, the former indicating no influence at all on the final result and the latter indicating that a particular datum is fixing one of the parameters. In Table 4 anorthite is flagged as being very influential, with a hat value four times larger (h_{an} = 0.54) than that of any other end-member, indicat-

TABLE 5. Average P-T and single end-member diagnostic information produced by Thermocalc for the RP13 assemblage with paragonite removed

	P	sd(P)	T	sd(T)	Cor	Fit	e^*	Hat
Lsq	7.2	0.4	538	10	0.742	1.10		
Mu	7.19	0.43	539	10	0.724	1.10	0.16	0.05
Cel	7.17	0.42	537	10	0.743	1.09	0.55	0.03
Phl	7.18	0.43	537	11	0.719	1.10	0.30	0.17
Ann	7.06	0.39	537	9	0.735	0.90	−1.86	0.06
East	7.19	0.43	538	10	0.741	1.10	−0.13	0.00
Clin	7.17	0.42	537	10	0.743	1.08	−0.52	0.03
Ames	7.21	0.42	539	10	0.737	1.09	0.47	0.10
Daph	7.10	0.44	535	11	0.773	1.08	−0.60	0.16
Gr	7.18	0.42	537	10	0.740	1.09	0.50	0.06
Py	7.20	0.44	538	10	0.761	1.10	−0.13	0.11
Alm	7.03	0.41	535	10	0.763	1.01	0.87	0.05
Andr	7.19	0.41	539	10	0.738	1.05	−1.00	0.03
An	7.57	0.56	541	10	0.706	1.04	0.66	0.56
Cz	7.42	0.45	541	10	0.757	1.03	−0.70	0.13
Ep	7.19	0.42	538	10	0.741	1.09	0.25	0.00
Cc	7.19	0.43	538	10	0.742	1.10	0	0
Q	7.19	0.43	538	10	0.742	1.10	0	0
H_2O	7.19	0.43	538	10	0.737	1.10	0.17	0.01
CO_2	7.31	0.42	542	10	0.765	1.03	−0.73	0.09

Note: for 95% confidence, fit (= σ_{fit}) should be <1.37.

ing that a change in the activity of anorthite causes a direct change in the average P-T. Our experience is that anorthite is often influential in thermobarometry, simply because it is a relatively low-density mineral that can contribute a large ΔV to reactions.

An obvious measure of outlying tendency is the activity residual, Δa_k, the difference between the measured activity of an end-member based on mineral analysis in a rock and the calculated activity required for all the equilibria to intersect at the average P-T (e.g. Powell, 1985a; Gordon, 1992). In Thermocalc output these activity residuals are normalized to the uncertainty on the measured activity and denoted e_k^* for end-member k, where e_k^* is defined by $\Delta a_k / \sigma_{a_k}$. Large values of e_k^* indicate that the corresponding activities are not being well fitted. An appropriate cutoff for e_k^* is given by the cumulative Stu-

dent's t distribution at the 99% level, with the number of degrees of freedom equaling the number of independent reactions minus two (for P-T) (Belsley et al., 1980, p. 20). So for six independent reactions, the cutoff is 3.8; for eight, 3.1; for ten, 2.9; and for 15, 2.65. This diagnostic should always be examined with reference to the influence of each end-member, as given by its hat value, h_k, because influential data, with large h_k, normally show small residuals, e_k^*, so that potentially damaging data may not be flagged by e_k^*.

The additional diagnostics used in Thermocalc to investigate the sensitivity of average P-T to the input data involve looking at the change in average P-T and the related statistics as a consequence of doubling the uncertainties on the input data, particularly the activities. The first six columns of diagnostics give the pressure, its un-

TABLE 6. Average P-T and single end-member diagnostic information produced by Thermocalc for the RP13 assemblage with paragonite and H_2O, CO_2 removed

	P	sd(P)	T	sd(T)	Cor	Fit	e^*	Hat
Lsq	7.4	1.1	540	64	0.959	0.95		
Mu	7.42	1.10	540	64	0.958	0.95	−0.03	0.01
Cel	6.87	1.26	505	74	0.969	0.87	0.82	0.29
Phl	7.65	1.18	553	68	0.964	0.92	0.41	0.10
Ann	7.16	1.12	531	64	0.956	0.79	−1.25	0.10
East	7.41	1.10	539	64	0.959	0.94	−0.27	0.00
Clin	7.40	1.10	539	64	0.959	0.94	−0.30	0.00
Ames	7.43	1.10	541	64	0.959	0.94	0.30	0.00
Daph	7.38	1.11	534	66	0.951	0.94	0.27	0.17
Gr	7.34	1.10	533	64	0.959	0.87	0.97	0.02
Py	8.18	1.41	581	79	0.974	0.88	−0.74	0.47
Alm	7.41	1.10	543	64	0.951	0.93	0.26	0.08
Andr	7.60	1.12	552	66	0.960	0.90	−0.80	0.08
An	7.46	1.12	538	64	0.915	0.94	0.12	0.38
Cz	7.45	1.10	538	64	0.950	0.93	−0.22	0.08
Ep	7.45	1.10	542	64	0.959	0.94	0.20	0.00
Q	7.42	1.10	540	64	0.959	0.95	0	0

Note: for 95% confidence, fit (= σ_{fit}) should be <1.42.

certainty, the temperature, its uncertainty, the P-T correlation coefficient, and the σ_{fit} that would result from doubling the uncertainties on each end-member. They are related to the deletion diagnostics of Belsley et al. (1980); deletion diagnostics are not used here because the deletion of end-members results in a change in the number of independent reactions, and thus the diagnostics cannot be calculated directly as part of the average P-T method. If an activity is inconsistent, then doubling its uncertainty changes the results; in particular, σ_{fit} and the uncertainties on average P-T decrease as the effect of the perturbing end-member is decreased. If an end-member is influential in the calculation, in the sense of being particularly indicative of conditions, then the uncertainties on average P-T increase on doubling the uncertainty on the activity of that end-member, because the influential end-member controls the calculation less. These various effects can be seen in Table 4, in which σ_{fit} fails the χ^2 test. Doubling the uncertainty on paragonite, already flagged by its large residual e^*_{pa}, causes obvious changes to the average P-T, decreasing the uncertainties on the average P-T, and strongly decreasing σ_{fit}. The effect of doubling its uncertainty is to lower σ_{fit} from 2.02 to 1.50. Removing paragonite altogether from the calculation, Table 5, brings σ_{fit} down to 1.10, where it now passes the χ^2 test. Further examination of the diagnostics is only for purposes of understanding the structure of the calculation, not to identify further outliers: the calculation is now consistent from a statistical point of view. We might note that annite has a slight degrading effect on the calculation, but, as χ^2 is passed, deleting it is not justified. If the uncertainties in the activities were to be made smaller, thus increasing σ_{fit} such that χ^2 were no longer passed, deleting annite would have the effect of changing the pressure and temperature only slightly (to $P = 7.0$ kbar, $T = 537$ °C), as its hat value is small. The hat for anorthite is still high, and we observe, as expected, that the pressure uncertainty would increase if the uncertainty on the activity of anorthite were to be doubled.

In practice, examination of the table of diagnostics, as in Tables 4–6, involves looking down the columns to note values of P and T that are significantly different from the average P-T. If these are associated with a significant decrease in σ_{fit}, there may be a case for removing the offending end-member from the analysis in a second calculation, but only in situations where the χ^2 test has failed. It is wise to delete single outliers, sequentially, in decreasing order of severity, until the χ^2 test is passed. In cases where the problem lies in general scatter rather than in an obvious small number of outliers, sequential deletion does not right the situation; in such cases the overall level of uncertainty on mineral activities may be suspect, and a case may be made for enlarging all the activity uncertainties and recalculating. Alternatively, the assemblage may reflect disequilibrium, partial retrogression, or constituent minerals grown during different metamorphic episodes in a complex tectonothermal history.

Deletion diagnostics can be calculated and can be very useful, but they need to be calculated either by separate applications of Thermocalc or by simulation through diagnostics generated with activity multiplied by some large number, not just multiplied by two. An obvious calculation for RP13 involves deleting the end-members, H_2O and CO_2 so that the results do not depend on the choice of fluid composition (Table 6). Note that the results are within the uncertainties of the full calculation, and that omitting H_2O and CO_2 causes the temperature to be poorly determined: devolatilization reactions normally act as thermometers. In the calculations for the tables and figures, $x_{H_2O} = 0.75$ and $x_{CO_2} = 0.25$ are used. There is no particular difficulty in extending the average P-T method to the calculation of fluid composition in addition to P-T, although that has not been implemented in Thermocalc yet. In the meantime, we suggest that an appropriate approach is to investigate the dependence of results on fluid composition, in the manner of Figure 8 in Powell and Holland (1988). In fact, the average fluid composition most likely corresponds to that with minimum σ_{fit} in PTX.

The relationship between average P-T, average P, and average T

When first performing average calculations on a rock, it is usually advisable to start by calculating average P at a series of temperatures (termed the average P locus), in the likely temperature range of formation of the rock. As observed by Powell (1985a) and Powell and Holland (1988), temperatures are usually known better than pressures, for example from the general phase relationships in the rock. If pressures are better known, then the average T at a series of pressures (the average T locus) can be calculated. The reason for starting by calculating a locus is that such calculations are more robust than for the average P-T, as only one variable is being solved for. Also they are simpler because average P (and average T) can be calculated directly without iteration (Powell and Holland, 1988, p. 196), unlike average P-T. Another reason for starting with average P or average T is that the average P-T point may be inaccessible. The inaccessibility of average P-T most often occurs when the uncertainty ellipse is large but extends into an acceptable range of conditions, with its center outside such a range. A common situation in which inaccessibility occurs is when all the well-constrained equilibria in a system have similar slopes. Then the uncertainty ellipse is cigar-shaped along this slope, and the average P-T is strongly correlated, with $\rho_{\bar{P},\bar{T}} \rightarrow \pm 1$. Another situation where inaccessibility occurs is when the equilibrium assemblage in a rock has been incorrectly identified. Starting with, for example, average P, for which the full range of diagnostics discussed above are given by Thermocalc, a nonequilibrium assemblage or other problems may be recognized and rectified in the simpler average P setting.

The relationship between the average P locus, the average T locus, and the average P-T (point) can be seen by using the expressions for the conditional density of the bivariate normal distribution (Morrison, 1976, p. 91–92),

which, in this context, involves looking at the covariance matrix for the average P-T:

$$\mathbf{V}_{\overline{P}\text{-}\overline{T}} = \begin{bmatrix} \sigma_{\overline{P}}^2 & \sigma_{\overline{P}\text{-}\overline{T}} \\ \sigma_{\overline{P}\text{-}\overline{T}} & \sigma_{\overline{T}}^2 \end{bmatrix}.$$

The consequence of fixing T at T' gives P' in terms of the P and T in the average P-T, $\overline{P}$, and $\overline{T}$ and the elements of this covariance matrix:

$$P' = \overline{P} + \frac{\sigma_{\overline{P}\text{-}\overline{T}}}{\sigma_{\overline{T}}^2}(T' - \overline{T})$$

and

$$\sigma_{P'}^2 = \sigma_{\overline{P}}^2 - \frac{\sigma_{\overline{P}\text{-}\overline{T}}^2}{\sigma_{\overline{T}}^2}.$$

This is none other than the equation for the average P and its uncertainty. It defines a line that runs through the average P-T point, having a slope of $\sigma_{\overline{P}\text{-}\overline{T}}/\sigma_{\overline{T}}^2$. Given the geometry of ellipses (e.g., Powell and Holland, 1988), the average P locus goes through the center of the ellipse defined by the above covariance matrix and the points on the boundary of the ellipse where $dP/dT = \infty$, Figure 6. In the same way, the average T locus goes through the center of the ellipse and the points on the boundary of the ellipse where $dP/dT = 0$.

DISCUSSION OF OTHER THERMOBAROMETRY METHODS

Several misconceptions have appeared in the recent literature regarding multiple reaction thermobarometry. The first is that the use of an independent set of reactions to calculate a unique P-T for equilibration (as in Powell and Holland, 1988, and in their computer program, Thermocalc) is inadvisable because different sets of independent reactions for a given mineral assemblage yield different results, as stated by Berman (1991, p. 836–837) and Gordon (1992, p. 1795). The second, allied to the first, is that the correlations among the reactions used in generating the P-T estimate need not be considered. In this paper we show that not only are such correlations fundamental, but also that it is only their omission that causes different independent sets of reactions to produce different results in the work of Gordon (1992) and Berman (1991).

In the individual species approach of Gordon (1992), he allows uncertainties in, and correlations between, the chemical potentials of the end-members. In contrast, we include, separately, the uncertainties on the activities and uncertainties and correlations on the enthalpies of formation. Apart from this, his method is formally identical to ours. However, the difference in the assignment of uncertainties is potentially significant, as the activity uncertainties are in the temperature-dependence part and the enthalpy uncertainties in the constant part of the chemical potential.

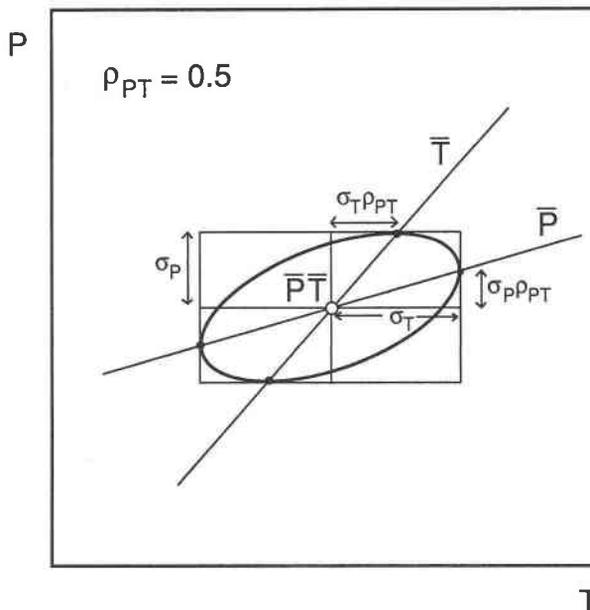In contrast to the Gordon and average P-T approaches, in TWEEQU (Berman, 1991), the problem of tackling

Fig. 6. The relation between the loci of average pressure $\overline{P}$ and average temperature $\overline{T}$ and the optimal average P-T point $\overline{P}$-$\overline{T}$. Calculated average pressures at fixed temperatures, e.g., Powell and Holland (1988), would lie along the line labeled $\overline{P}$, whereas calculated average temperatures at fixed pressures would lie along the line labeled $\overline{T}$. These relations are identical to those obtained by linear regression of a cloud of P-T points, with $\overline{P}$ representing regression of P on T and $\overline{T}$ representing regression of T on P.

overdetermined systems of equilibria to estimate P-T is solved by performing a weighted average of the P-T positions of all the intersections involving all of the reactions in the system. No correlations are included; instead, a semiempirical scheme is used to weight the influence on the averaging of potentially poorly constrained intersections. Unfortunately the method does not compensate for the omitted correlations because the implied movement of the reactions to make them intersect at the estimated P-T is dependent on the correlations among the positions of the reactions. Whereas TWEEQU generally gives calculated P-T values similar to those of the average P-T method, it need not always do so because of this dependence.

REFERENCES CITED

Belsley, D.A., Kuh, E., and Welsch, R.E. (1980) Regression diagnostics, 292 p. Wiley, New York.
Berman, R.G. (1988) Internally-consistent thermodynamic data for minerals in the system Na_2O-K_2O-CaO-MgO-FeO-Fe_2O_3-Al_2O_3-SiO_2-TiO_2H$_2$O-CO_2. Journal of Petrology, 29, 445–522.
——(1991) Thermobarometry using multi-equilibrium calculations: A

new technique, with petrological applications. Canadian Mineralogist, 29, 833–855.

Essene, E.J. (1989) The current status of thermobarometry in metamorphic rocks. Geological Society Special Publication, 43, 1–44.

Ghent, E.D., and Stout, M.Z. (1981) Geothermometry and geobarometry and fluid compositions of metamorphosed calc-silicates and pelites, Mica Creek, British Columbia. Contributions to Mineralogy and Petrology, 76, 92–97.

Ghent, E.D., Robbins, D.B., and Stout, M.Z. (1979) Geobarometry and geothermometry of plagioclase-biotite-garnet-muscovite assemblages. American Mineralogist, 64, 874–885.

Gordon, T.M. (1992) Generalized thermobarometry: Solution of the inverse chemical equilibrium problem using data for individual species. Geochimica et Cosmochimica Acta, 56, 1793–1800.

Helgeson, H.C., Delaney, J.M., Nesbitt, H.W., and Bird, D.K. (1978) Summary and critique of the thermodynamic properties of rock-forming minerals. American Journal of Science, 278-A, 1–229.

Holland, T.J.B., and Powell, R. (1985) An internally consistent thermodynamic dataset with uncertainties and correlations. II. Data and results. Journal of Metamorphic Geology, 3, 343–370.

—— (1990) An internally consistent thermodynamic dataset with uncertainties and correlations: The system Na$_2$O-K$_2$O-CaO-MgO-MnO-FeO-Fe$_2$O$_3$-Al$_2$O$_3$-SiO$_2$-TiO$_2$-C-H$_2$-O$_2$. Journal of Metamorphic Geology, 8, 89–124.

Kohn, M.J., and Spear, F.S. (1991) Error propagation for barometers. II. Application to rocks. American Mineralogist, 76, 138–147.

Lieberman, J., and Petrakakis, K. (1991) TWEEQU thermobarometry: Analysis of uncertainties and applications to granulites from western Alaska and Austria. Canadian Mineralogist, 29, 857–887.

Mikhail, E.M. (1976) Observations and least squares, 321 p. Dun-Donnelly, New York.

Morrison, D.F. (1976) Multivariate statistical methods, 415 p. McGraw-Hill, New York.

Powell, R. (1978) Equilibrium thermodynamics in petrology, 284 p. Harper and Row, London.

—— (1985a) Geothermometry and geobarometry: A discussion. Journal of the Geological Society of London, 142, 29–38.

—— (1985b) Regression diagnostics and robust regression in geothermometer/geobarometer calibration: The garnet-clinopyroxene geothermometer revisited. Journal of Metamorphic Geology, 3, 231–243.

Powell, R., and Holland, T.J.B. (1985) An internally consistent thermodynamic dataset with uncertainties and correlations. I. Methods and a worked example. Journal of Metamorphic Geology, 3, 327–342.

—— (1988) An internally consistent thermodynamic dataset with uncertainties and correlations. III. Application methods, worked examples and a computer program. Journal of Metamorphic Geology, 6, 173–204.

Richardson, S.W., and Powell, R. (1976) Thermal causes of the Dalradian metamorphism in the Central Highlands of Scotland. Scottish Journal of Geology, 12, 237–268.

Appendix 1. The calculation of average temperatures and pressures

The purpose of this appendix is to outline the method of calculating average pressures and temperatures, $\overline{P}$-$\overline{T}$. This involves finding a P-T (the $\overline{P}$-$\overline{T}$) that minimizes, in a least-squares sense, the amount that the input data must be varied for $0 = \Delta G^0 + RT \ln K$ for each of the reactions in the independent set to be consistent. According to Powell and Holland (1988), the sources of uncertainty in the input data are the enthalpies of formation and activities of the end-members. To clarify and simplify the discussion, the equilibrium relationships may be linearized

as $0 = \Delta H_R - T\Delta S_R + P\Delta V_R + RT \ln K$ giving

$$P = \left(-\frac{\Delta H_R}{\Delta V_R}\right) + \left(\frac{\Delta S_R - R \ln K}{\Delta V_R}\right)T \equiv a + bT.$$

In this, a is uncertain primarily through uncertainties in the enthalpies of formation, and b is uncertain primarily through uncertainties in the activities. We denote $\mathbf{h}$, the (column) vector of enthalpies of formation of the end-members, $\mathbf{k}$, the (column) vector of $R \ln a_i$ (the gas constant, R, times the natural logarithms of the activities of the end-members in the phases), and $\mathbf{R}$, the matrix of reaction coefficients for the independent set of reactions, each row of $\mathbf{R}$ corresponding to a reaction. Then, the vector of enthalpies of reaction, ΔH_R, for the independent set of reactions is $\mathbf{Rh}$, and the vector of $R \ln K$ values is $\mathbf{Rk}$. The following development is simplified by adopting the following definitions:

$$\mathbf{z} \equiv \begin{bmatrix} \mathbf{h} \\ \mathbf{k} \end{bmatrix}$$

and

$$\theta \equiv \begin{bmatrix} P \\ T \end{bmatrix}.$$

The uncertainties on $\mathbf{z}$, in the form of a covariance matrix, are

$$\mathbf{V} = \begin{bmatrix} \mathbf{V_h} & 0 \\ 0 & \mathbf{V_k} \end{bmatrix}.$$

$\mathbf{V_h}$ and $\mathbf{V_k}$ are the covariance matrices of $\mathbf{h}$ and $\mathbf{k}$, whose diagonal elements are the squares of the standard deviations (the variances) of the elements of $\mathbf{h}$ and $\mathbf{k}$, and the off-diagonal elements are the covariances between the elements. $\mathbf{V_k}$ is normally diagonal (activities are uncorrelated), whereas $\mathbf{V_h}$, as generated by the least-squares method of data extraction (Powell and Holland, 1985), is full.

Finding the optimal $\overline{P}$-$\overline{T}$ can be envisaged in terms of minimizing the sum of squares of the weighted differences between measured and estimated enthalpies and ln activities:

$$(\mathbf{z} - \hat{\mathbf{z}})^T \mathbf{V}^{-1} (\mathbf{z} - \hat{\mathbf{z}}) \qquad (A1)$$

subject to the constraints that the equilibrium relationships for each of the independent reactions give the same average P-T:

$$\overline{P}\mathbf{1} = \hat{\mathbf{a}} - \hat{\mathbf{b}}\overline{T} \qquad (A2)$$

where $\mathbf{z}$ is a measured value and $\hat{\mathbf{z}}$ is an estimated value, corresponding to the estimated values of average P and T. The $\hat{\mathbf{a}}$ and $\hat{\mathbf{b}}$ are estimated values of $\mathbf{a}$ and $\mathbf{b}$ calculated from $\hat{\mathbf{z}}$. A column vector of ones is denoted $\mathbf{1}$.

The solution of this type of problem is covered by Mikhail (1976, p. 111–117), the critical step being the linearization of the constraints with respect to θ and $\mathbf{z}$. Because the constraints are nonlinear, finding $\overline{P}$ and $\overline{T}$ (and $\hat{\mathbf{a}}$ and $\hat{\mathbf{b}}$) must be iterative. Therefore the aim is to find equations to express the change in θ, $\Delta\theta$, and the change in $\mathbf{z}$,

Δz, for each iteration, so that convergence occurs to a solution at which Equation A1 is minimized and Equation A2 is satisfied. For such iterative sequences, a starting guess is required: measured values can be used for z, from which a and b can be calculated, and geological intuition can be used for θ, i.e., P and T.

Writing the constraints as $F = -P1 + a + bT$, and noting that $F = 0$ corresponds to the constraints being satisfied, we may write:

$$A \equiv \frac{\partial F}{\partial z} = SR[1 \ T 1]$$

and

$$B \equiv \frac{\partial F}{\partial \theta} = [-1 \ b]$$

where S is a diagonal matrix whose diagonal elements are the negative reciprocals of the pressure dependence of ΔG^0 at the average P-T for the reactions in the independent set. Then, following Mikhail (p. 114), the change in θ at each iteration, $\Delta \theta$, is

$$\Delta \theta = [B^T(AVA^T)^{-1}B]^{-1}B^T(AVA^T)^{-1}f$$

in which the only new term is f, defined as $f = -\overline{P}1 + a + b\overline{T}$, the departure from the constraints for the current $\overline{P}$-$\overline{T}$ with the a and b calculated with the measured z. It is convenient to reexpress $\Delta \theta$, using $X \equiv D^+B$ and $e \equiv D^+f$, with $D \equiv V^{1/2}A^T$:

$$\Delta \theta = X^+e$$

the plus superscript denotes the pseudoinverse, $X^+ = (X^TX)^{-1}X^T$ (for full rank X) (e.g., Powell, 1985b, p. 233). In practice, X^+ (and $V^{1/2}$) are calculated with a singular value decomposition. In the definition of e and X, D^+ acts as a projection from reaction space to data space; thus, whereas f is a residual on the reactions in the independent set, e is the residual on the input data.

The change in z at each iteration, Δz, is

$$\Delta z = V^{1/2}X^+(-\overline{P}1 + \hat{a} + \hat{b}\overline{T}).$$

The term in brackets is just the departure from the constraints for the current P-T and $\hat{z}$. At the end of each iteration, θ and $\hat{z}$ are incremented with the newly calculated $\Delta \theta$ and Δz. Iteration proceeds until $\Delta \theta$ and Δz approach zero, the former when the objective function is minimized, the latter when the constraints are obeyed. This rarely takes more than four iterations, and techniques to ensure convergence are unnecessary because the problem is nearly linear. At the solution, the σ_{fit} is

$$\sigma_{fit}^2 = \frac{f^T(D^TD)^{-1}f}{r - 2}$$

representing the scatter of the data around the solution; it is the statistic that can be used in a χ^2 test to determine if the input data should in fact be combined to calculate an average P-T (see text). The uncertainties on the av-

erage are given by

$$V_\theta = \sigma_{fit}^2(X^TX)^{-1} = \begin{bmatrix} \sigma_{\overline{P}}^2 & \sigma_{\overline{P}\cdot\overline{T}} \\ \sigma_{\overline{P}\cdot\overline{T}} & \sigma_{\overline{T}}^2 \end{bmatrix}.$$

In this expression, σ_{fit} is set to 1 if $\sigma_{fit} < 1$, otherwise V_θ is too optimistic. The residuals on the data, $e = D^+f$, and the diagonal elements of the hat matrix, $H = X(X^TX)^{-1}X^T$, are used in Appendix 2, and are referred to in the text.

APPENDIX 2. DIAGNOSTICS FOR AVERAGE TEMPERATURES AND PRESSURES

Diagnostics allow an appraisal of the sensitivity of the calculated average P-T on the input data. To do this it is necessary to linearize the problem at the solution, or, equivalently, to make a linear problem with the properties of the real nonlinear problem at the solution. This and the following development use the notation of Appendix 1 with values at the solution, in particular:

$$X = (V^{1/2}A^T)^+B. \tag{A3}$$

The linear problem can be written as $\theta = X^+y$. The diagnostics chosen here to investigate sensitivity involve looking at the change in average P-T and the related statistics as a consequence of doubling the uncertainties on the input data, particularly the activities, k. Doubling the uncertainty of an activity amounts to replacing V in Equation A3 by $V^{1/2}W^2V^{1/2}$, where W is a diagonal weighting matrix whose diagonal elements are one, except for the end-member of interest whose element is two, to double that uncertainty. Then, following the logic in Belsley et al. (1980), with $D_w = WV^{1/2}A^T$, and, after some manipulation, θ for a particular, W, θ_w, is given by

$$\theta_w = \theta - \beta e_i(X^+)_i$$

where i is the index of the nonunit diagonal element in W, $(X^+)_i$ is the ith column of X^+, e_i is the ith element of e defined above, and

$$\beta = \frac{1}{\frac{1}{1 - w_i^2} + h_i - h_i'}$$

in which $h_i = X_i(X^TX)^{-1}X_i^T$ and $h_i' = (D_w)_i(D_w^TD_w)^{-1} \cdot (D_w^T)_i$, and $w_i = 2$ for doubling uncertainties. These rules are diagonal elements of projection matrices involved in the analysis. Analogously

$$V_{\theta_w} = \frac{\sigma_w^2}{\sigma^2}[V_\theta - \beta(X^+)_i(X^{+T})_i]$$

and

$$\sigma_w^2 = \sigma^2 + \frac{\beta e_i^2}{r - 2}$$

where, again, σ_w^2 in V_{θ_w} is set to unity if $\sigma_w < 1$.

Note that these diagnostics may be calculated with little computational effort from terms $(D, X, \ldots)$ in the calculation of the average P-T itself.